NANO LETTERS

Letter

pubs.acs.org/NanoLett

Probing Symmetry Properties of Few-Layer MoS_2 and h-BN by Optical Second-Harmonic Generation

Yilei Li,[†] Yi Rao,[‡] Kin Fai Mak,[†] Yumeng You,[†] Shuyuan Wang,[†] Cory R. Dean,[§] and Tony F. Heinz*[,†]

[†]Departments of Physics and Electrical Engineering, Columbia University, 538 West 120th Street, New York, New York 10027, United States

[‡]Department of Chemistry, Columbia University, 3000 Broadway, New York, New York 10027, United States

[§]Department of Physics, The City College of New York, 160 Convent Avenue, New York, New York 10031, United States

Supporting Information

ABSTRACT: We have measured optical second-harmonic generation (SHG) from atomically thin samples of MoS_2 and h-BN with one to five layers. We observe strong SHG from materials with odd layer thickness, for which a noncentrosymmetric structure is expected, while the centrosymmetric materials with even layer thickness do not yield appreciable SHG. SHG for materials with odd layer thickness was measured as a function of crystal orientation. This dependence reveals the rotational symmetry of the lattice and is shown to provide a purely optical method of determining the orientation of crystallographic axes. We report values for the nonlinearity of monolayers and odd-layers of MoS_2 and h-BN and compare the variation as a function of layer thickness with a model that accounts for wave propagation effects.

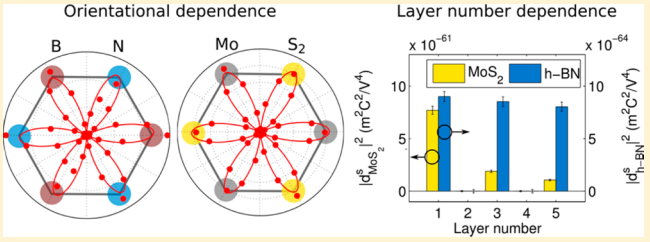

KEYWORDS: *Molybdenum disulfide, hexagonal boron nitride, optical second-harmonic generation, symmetry, crystallographic orientation*

In atomically layered materials, the individual layers will generally exhibit different symmetry from the corresponding bulk crystals. Few-layer materials of different layer thickness can moreover have distinct symmetries from one another, even when their thickness differs by only one atomic layer. Since symmetry plays a critical role in defining the material properties, such differences in symmetry lead to significant differences in material properties. Among the layered materials, few-layer graphene, MoS_2, and hexagonal BN have attracted great interest due to their distinctive properties and potential for novel applications. Monolayer graphene is a semimetal without a band gap. However, in bilayer graphene, a sizable band gap can be opened when inversion symmetry is lifted by an out-of-plane electric field.[1−4] Single-layer MoS_2 and h-BN are noncentrosymmetric materials, while their bilayers and bulk counterparts are expected to exhibit inversion symmetry. The broken inversion symmetry in transition metal dichalcogenides of single-layer thickness has been shown to permit the production of long-lived valley polarization by optical helicity.[5−7] It has also been predicted that the noncentrosymmetric single-layer sheets will exhibit a strong intrinsic piezoelectric response.[8−11]

Bulk MoS_2 is built from layers consisting of two hexagonal lattices of S atoms and a sheet of Mo atoms occupying trigonal prismatic sites between the S sheets (Figure 1a). Bulk h-BN is formed from layers of honeycomb lattices of B and N atoms, occupying, respectively, the A and B sublattices in each layer (Figure 1b). Both MoS_2 and h-BN layers are stacked in 2H order, with pairs of layers forming a unit that is repeated along the *c*-axis.[12,13] Because of their similar structure, bulk MoS_2 and h-BN crystals belong to the same centrosymmetric D_{6h}^4 space group. However, few-layer segments of the bulk crystal will generally exhibit different symmetry properties. In the case of few-layer MoS_2 and h-BN, slices of even layer thickness belong to the centrosymmetric D_{3d}^3 space group, while slices of odd layer thickness belong to the noncentrosymmetric D_{3h}^1 space group. It has been demonstrated that stable few-layer units of both of these materials can be isolated by mechanical exfoliation.[14] Since the surface of a bulk crystal can undergo lattice reconstruction, whether these isolated atomically thin sheets exhibit the varying crystallographic symmetries expected from their bulk parents is a question of fundamental scientific interest.

In this work, we probe the symmetry variations in few-layer MoS_2 and h-BN by optical second-harmonic generation (SHG). The SHG process, which is described in the electric-dipole approximation by a third-rank tensor, is known to be a sensitive probe of symmetry of surface layers.[15−17] Using this method, we verify that inversion symmetry is indeed broken in MoS_2 and h-BN samples of odd layer thickness. This is manifested by the large enhancement of the second-harmonic

Received: April 29, 2013
Revised: May 22, 2013
Published: May 29, 2013

   dx.doi.org/10.1021/nl401561r | *Nano Lett.* 2013, 13, 3329−3333

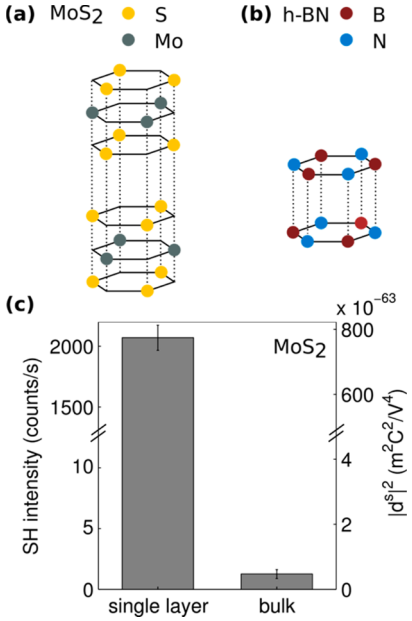

Figure 1. (a,b) Structure of repeating two-layer units in 2H-stacked MoS_2 and h-BN. (c) The SH intensity and surface nonlinear susceptibility for single-layer MoS_2 and from the surface of bulk MoS_2. The vertical axes are broken to allow the display of the very different SH response from the single-layer and bulk material.

(SH) response of these samples compared both to samples of even numbers of layers and to the bulk crystals.[18] The three-fold rotational symmetry of the layered materials (for odd numbers of layers) was probed by the orientational dependence of SH intensity. In this manner, we establish SHG as a precise optical probe of the orientation of the crystallographic axes. A recent study clearly demonstrated the orientational dependence of SHG from single-layer MoS_2 and applied this sensitivity to imaging crystal domains in monolayer MoS_2 samples grown by chemical vapor deposition.[19] (After the submission of our paper, ref 20 discussing symmetry variations in tungsten dichalcoginde and ref 21 discussing SHG from MoS_2 layers appeared in the literature.[20,21]) Our findings further indicate that the isolated few-layer MoS_2 and h-BN retain the crystallographic structure of the layers in the bulk crystals. For odd-layer MoS_2 and h-BN samples, we further determine the absolute strength of the SH susceptibility and study its evolution with layer thickness. To describe the different behavior observed for the two material systems with layer thickness, we introduce a model accounting for the phase shift and absorption of the optical fields. In MoS_2, the interlayer electronic coupling and the corresponding change in electronic structure as a function of layer thickness are found to be of importance in defining the linear and nonlinear response.

We prepared few-layer MoS_2 and h-BN samples on fused silica substrates using mechanical exfoliation.[14] The layer thicknesses of the different exfoliated MoS_2 samples were determined by the central wavelength and intensities of the photoluminescence from the direct gap (for monolayers) and from indirect band gap transition (for thicker samples).[22,23] For analysis of the h-BN samples, we relied on the relative intensity of the Raman peak of E_{2g} optical phonon mode near 1370 cm^{-1},[24] confirming our assignments of layer thickness by measurements with atomic-force microscopy (AFM).

The SH measurements were performed in a reflection geometry using normal incidence excitation. The pump radiation was supplied by a mode-locked Ti:sapphire oscillator operating at an 80 MHz repetition rate. The pulses were of 90 fs duration and centered at a wavelength of 810 nm. Using a 100× objective, we focused the pump radiation to a spot size of about 1 μm on the sample. For measurements of MoS_2, we limited the average laser power to 1 mW; for measurements of h-BN, laser powers up to 10 mW were employed. The retroreflected SH signal was collected by the same objective, separated by a beam splitter and filtered to block reflected fundamental radiation. An analyzer was used to select the polarization components of the SH radiation lying either parallel or perpendicular to the polarization of the pump beam. The SH signal was detected by a thermoelectrically cooled CCD camera after it was dispersed in a spectrometer. The SH character of the detected radiation was verified by its wavelength and quadratic power dependence on the pump intensity. In our setup, we could freely rotate the samples to obtain the orientational dependence of the SH response.

We describe the second-order nonlinear response from the various single- and few-layer samples in terms of a surface nonlinear susceptibility tensor $\mathbf{d}^s$ that relates the applied laser field to the induced nonlinear sheet polarization in the sample. Calibrated values of the second-order nonlinear coefficients for few-layer MoS_2 and h-BN samples were obtained by comparing the corresponding SH intensity I_s to the reference SH intensity I_r from the surface of a z-cut bulk crystal of α-quartz. For this measurement, the quartz crystal was oriented so that its largest SH coefficient (d_{11}) was accessed. We then determined the relevant element of the surface second-order nonlinear response d^s from the ratio I_s/I_r using the relation

$$\frac{d^s}{d_{11}} = \frac{c}{4\omega[n(\omega) + n(2\omega)]}\sqrt{\frac{I_s}{I_r}} \quad (1)$$

Here ω is the fundamental (angular) frequency, and $n(\omega)$ and $n(2\omega)$ represent the (ordinary) refractive indices of crystalline quartz at the fundamental and SH frequencies, respectively. Equation 1 is derived by taking the ratio of an analytic expression for the SH intensity produced by a 2D polarizable sheet on a semi-infinite dielectric substrate[25] to that produced by the boundary of a semi-infinite nonlinear medium with a bulk second-order response.[26] It should be noted that the surface nonlinear response is expected to be a complex quantity for the (resonant) MoS_2 samples. We did not determine the phase of the response, and d^s should be understood as the modulus of the complex surface nonlinear susceptibility.

The dramatic role of symmetry can be seen in the contrast of the SH response of a monolayer of MoS_2 and of the bulk MoS_2 crystal. We observed an increase in the reflected SH intensity by more than a thousand times for the monolayer compared to the surface of the bulk material (Figure 1c). This enhancement reflects the fact that bulk MoS_2 is centrosymmetric, and previous studies have shown it to have a very weak SH response.[18] The origin for the small, but finite SH signal from bulk MoS_2 is discussed below.

For both the parallel and perpendicular polarization components, the SH intensity from single-layer MoS_2 exhibited a strongly varying, six-fold symmetric response as a function of azimuthal angle for rotation about its surface normal (Figure 2).[27] Similar results were obtained for single-layer h-BN samples (Supporting Information). On the basis of the

dx.doi.org/10.1021/nl401561r | Nano Lett. 2013, 13, 3329−3333

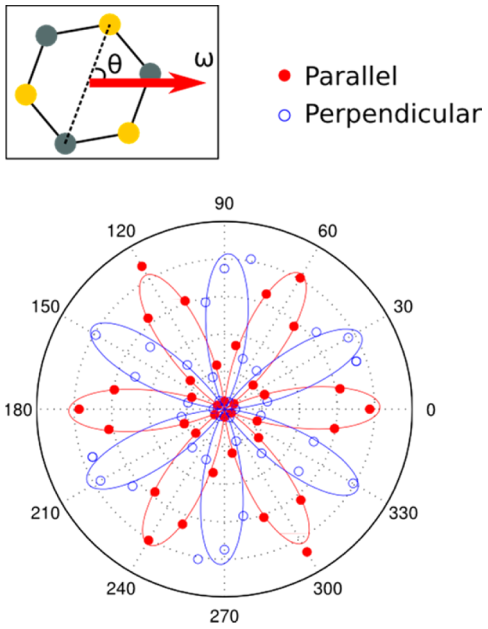

Figure 2. Polar plot of the SH intensity from single-layer MoS_2 as a function of the crystal's azimuthal angle θ. The SH radiation components detected parallel (red) and perpendicular (blue) to the polarization of the fundamental field are shown. The symbols are experimental data[27] and the solid lines are fits to the symmetry analysis described in the text. The angle $\theta = 0$ corresponds to an orientation where the polarization of the pump beam lies along a mirror plane of the crystal, as shown in the inset.

structure of the bulk crystal, as discussed above, exfoliated monolayers of both MoS_2 and h-BN are expected to belong to the D_{3h}^1 symmetry group. For this case, we expect only one independent nonvanishing element of the nonlinear response: $d^s = d^s_{yyy} = -d^s_{yxx} = -d^s_{xxy} = -d^s_{xyx}$.[28] This symmetry information determines the dependence of the two polarization components of SH response on sample orientation:

$$I_{\parallel} = I_0 \cos^2(3\theta) \qquad (2)$$

$$I_{\perp} = I_0 \sin^2(3\theta)$$

Here θ denotes the angle between the mirror plane in the crystal structure and the polarization of the pump beam, and I_0 is the maximum intensity of the SH response. As shown in Figure 2, the experimental data agree well with these predicted expressions for the angular variation. The same orientational dependence of the SH intensity was also observed in MoS_2 and h-BN with 1, 3, and 5 layers (Supporting Information), precisely as expected based on the identical space group for all of these materials. We note that the dependence of SH electric field (not the SH intensity) on crystallographic orientation actually exhibits three-fold rotational symmetry, in accordance with the lattice symmetry.

From the intensity maxima in the previous measurement and known SH nonlinear susceptibility for quartz of $d_{11} = 2.7 \times 10^{-24}$ C/V^2 (7.4×10^{-10} esu),[29] we obtain for single-layer MoS_2 and h-BN values of the surface nonlinear susceptibility of $d^s_{MoS2} = 8.8 \times 10^{-31}$ m·C/V^2 (2.4×10^{-14}esu) and $d^s_{h\text{-}BN} = 3.0 \times 10^{-32}$ m·C/V^2 (8.3×10^{-16} esu). The effective volume second-order nonlinear susceptibilities for MoS_2 and h-BN are then $d_{MoS2} = 1.4 \times 10^{-21}$ C/V^2 and $d_{h\text{-}BN} = 9.1 \times 10^{-23}$ C/V^2. Here we have assumed effective thicknesses of the layers of $t_{MoS2} = 0.62$ nm[12] and $t_{h\text{-}BN} = 0.33$ nm,[13] corresponding to the layer separation in the bulk materials. The effective nonlinear susceptibility of h-BN is seen to be comparable to that of common transparent nonlinear crystals such as $LiNbO_3$ and β-BaB_2O_4. Because of resonant enhancement, the MoS_2 monolayer has an effective nonlinear susceptibility that is 1 order of magnitude larger, similar to that of absorbing nonlinear crystals such as GaAs and Te.[30]

For few-layer h-BN, strong SH radiation with similar intensity occurs for odd numbers of layers, while even numbers of layers do not show measurable SHG (Figure 3a). The intensity values for different layer thicknesses were taken at the lattice orientations corresponding to the peak SH response. The signal for even numbers of layers is at most 2% of that emitted from the single layer. This large suppression of SH radiation in even numbers of layers shows that these structures do indeed exhibit inversion symmetry, as expected from the bulk crystal.

To understand the thickness dependence of the SHG response more quantitatively, we introduce a simple model of the expected response based on electronically decoupled layers, but that still accounts for electromagnetic propagation effects at both the fundamental and SH frequencies. In computing phase shifts and absorption, we assume the thin slabs to have the same linear dielectric constants as their bulk counterparts.[31,32] In addition to propagation through the sample material, we also

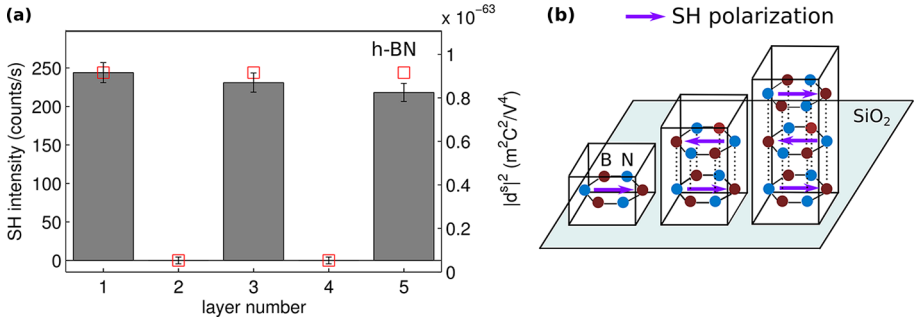

Figure 3. (a) The layer dependence of SH intensity and surface nonlinear susceptibility for few-layer h-BN. The histogram shows the experimental results, with uncertainties indicated by the error bars. The red squares display the results of a model (described in the text) that considers the phase evolution of the fundamental and SH fields, but neglects changes in the electronic structure from interlayer coupling. The model is calibrated to the results for the single-layer sample. (b) Illustration of the model for the calculation of the SH intensity as a function of layer thickness. The individual layers of h-BN are approximated as thin slabs and the polarization is assumed to be generated at the center of each layer. The alternating orientation of successive layers leads to an alternation in the nonlinear susceptibility of each layer.

dx.doi.org/10.1021/nl401561r | Nano Lett. 2013, 13, 3329−3333

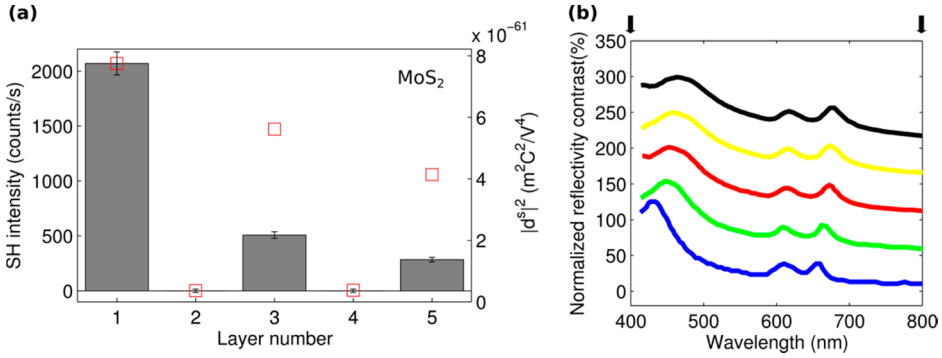

Figure 4. (a) The layer dependence of SH intensity and surface nonlinear susceptibility for few-layer MoS_2 samples. The histogram shows the experimental results, with uncertainties indicated by the error bars. The red squares show the results of the model (described in the text) that has been applied for h-BN, but now also includes the effect of absorption of the fundamental and SH fields. (b) The relative change of reflectance of few-layer MoS_2 samples on a fused silica substrate. Successive spectra from the bottom to the top correspond to 1−5 layers. The spectra have been normalized for layer thickness. For clarity, the spectra have also been displaced vertically by 50 percentage units for each additional layer. The arrows indicate the wavelengths of fundamental and SH photons. (Based on Figure S1a in the Supporting Information of ref 22).

include the influence of the reflection of both the fundamental and SH fields from the underlying substrate. The SH radiation from each layer is calculated taking into account the alternating sign of the SH susceptibility in adjacent layers (Figure 3b). As shown Figure 3a, the model captures the dramatic reduction in SHG in samples of even layer thickness. For two layers, for example, the model predicts a SH response that is just 0.008% of that from a monolayer. The nonzero result arises from the small but finite optical phase shift between the layers, which acts to prevent complete cancellation. This effect corresponds formally to the inclusion of nonlinear response beyond the electric-dipole approximation in orders of spatial nonlocality. For odd layer numbers N, in the simplest picture, the signal from a block of $N - 1$ layers fully cancels out, leaving the residual signal from just one layer. Thus, no thickness dependence would be expected. The aforementioned propagation effects in the transparent h-BN system modify this expectation only very slightly. The predicted signal from five layers is, for example, 99.8% of that from a monolayer, in reasonable agreement with the experimental results.

For the case of MoS_2, we again observed strong enhancement of the SH intensity in odd numbers of layers compared to the response for even numbers of layers. The SH intensity from odd numbers of layers, however, decreases significantly from one layer to five layers (Figure 4a), in contrast to the nearly constant response for h-BN. Because the band gap of MoS_2 is smaller than the SH photon energy, we expect light absorption to play a significant role. We applied the model described above to determine the expected influence of these propagation effects, including attenuation (Figure 4a). The results are in agreement with the experimental trends for the variation of the SH intensity with layer thickness. The model, however, underestimates the decrease in SHG actually observed with increasing layer thickness. The additional reduction can be attributed to interlayer coupling. These effects modify the electronic structure of few-layer MoS_2 and induce further changes in the linear and nonlinear susceptibilities. The evolving electronic structure with layer number for few-layer MoS_2 is demonstrated by reflectivity contrast measurements (Figure 4b). In particular, the change of resonance feature close to 2ω can have a substantial effect on both the linear response and the SH susceptibility of few-layer MoS_2.[28] In the limit of a bulk crystal, the strong, but imperfect, cancellation of SHG from neighboring layers leads to a weak, but finite, SH response. This response is expected even without accounting for any change (symmetry lowering) in the inherent properties of the top monolayer of material, the effect typically considered in analysis of surface SHG.[17] Our simple model predicts the bulk SH response to be 0.20% of that of a monolayer, comparable to the experimentally observed ratio.

The SH probe has several useful properties for characterizing few-layer MoS_2 and h-BN materials. First, the high contrast of SH intensities between even and odd numbers of layers can be used to supplement other optical characterization tools of layer number. The method is distinctive in providing strong contrast between single and bilayer samples. For MoS_2 with odd numbers of layers, even the exact layer number can be determined from the strong variation of SH intensity with layer number. Second, from the dependence of the SHG on the orientation of the crystal, we can determine the orientation of the crystallographic axes for odd-layer MoS_2 and h-BN. This purely optical method requires minimal sample preparation, is noninvasive, and imposes no special environmental requirements. Third, owing to the strong SH response for odd number of layers of MoS_2, the approach can be used for high throughput spatial mapping of domain orientation in polycrystalline samples, like those recently synthesized by chemical vapor deposition.[19,33−36]

In conclusion, we have experimentally probed the symmetry properties of few-layer MoS_2 and h-BN by optical second-harmonic generation. We verified that the few-layer samples retain the lattice symmetry they possess as part of the bulk material. The strong enhancement of SH intensity for odd numbers of layers compared to even numbers of layers shows that samples of even layer thickness possess inversion symmetry, while inversion symmetry is broken for odd layer thickness. The expected layer dependence of SH intensity from few-layer MoS_2 and h-BN was considered within a model accounting for wave propagation effects. Good agreement with the measured layer dependence was obtained for few-layer h-BN, but only the correct trend was predicted for few-layer MoS_2. The discrepancy between the model and experiment for MoS_2 indicates the importance of the material's evolving electronic structure with layer thickness as a result of interlayer electronic coupling. The orientational dependences of the SH intensity from MoS_2 and h-BN for odd layer thickness is consistent with the three-fold rotational symmetry of the lattice

dx.doi.org/10.1021/nl401561r | Nano Lett. 2013, 13, 3329−3333

and was demonstrated to be a useful tool for the determination of the orientation of the material's crystallographic axes.

■ ASSOCIATED CONTENT

Supporting Information

This work was supported by the National Science Foundation under Grant DMR-1124894 (for h-BN studies) and by the Department of Energy, Office of Basic Energy Sciences under Grant DE-FG02-07ER15842(for MoS_2 studies) and under Grant DE-SC0001085 for optical instrumentation at Columbia University's EFRC for Re-Defining Photovoltaic Efficiency through Molecule Scale Control.

This material is available free of charge via the Internet at http://pubs.acs.org.

■ AUTHOR INFORMATION

Corresponding Author

*E-mail: tony.heinz@columbia.edu.

Notes

The authors declare no competing financial interest.

■ REFERENCES

(1) Castro, E. V.; Novoselov, K. S.; Morozov, S. V.; Peres, N. M. R.; dos Santos, J. M. B. L.; Nilsson, J.; Guinea, F.; Geim, A. K.; Neto, A. H. C. *Phys. Rev. Lett.* **2007**, *99* (21), 216802.
(2) Zhang, Y.; Tang, T.-T.; Girit, C.; Hao, Z.; Martin, M. C.; Zettl, A.; Crommie, M. F.; Shen, Y. R.; Wang, F. *Nature* **2009**, *459* (7248), 820−823.
(3) Mak, K. F.; Lui, C. H.; Shan, J.; Heinz, T. F. *Phys. Rev. Lett.* **2009**, *102* (25), 256405.
(4) Ohta, T.; Bostwick, A.; Seyller, T.; Horn, K.; Rotenberg, E. *Science* **2006**, *313* (5789), 951−954.
(5) Cao, T.; Wang, G.; Han, W.; Ye, H.; Zhu, C.; Shi, J.; Niu, Q.; Tan, P.; Wang, E.; Liu, B.; Feng, J. *Nat. Commun.* **2012**, *3*, 887.
(6) Mak, K. F.; He, K.; Shan, J.; Heinz, T. F. *Nat. Nanotechnol.* **2012**, *7* (8), 494−498.
(7) Zeng, H.; Dai, J.; Yao, W.; Xiao, D.; Cui, X. *Nat. Nanotechnol.* **2012**, *7* (8), 490−493.
(8) Duerloo, K.-A. N.; Ong, M. T.; Reed, E. J. *J. Phys. Chem. Lett.* **2012**, *3* (19), 2871−2876.
(9) Duerloo, K.-A. N.; Reed, E. J. *Nano Lett.* **2013**, *13* (4), 1681−1686.
(10) Michel, K. H.; Verberck, B. *Phys. Rev. B* **2009**, *80* (22), 224301.
(11) Michel, K. H.; Verberck, B. *Phys. Rev. B* **2011**, *83* (11), 115328.
(12) Wilson, J. A.; Yoffe, A. D. *Adv. Phys.* **1969**, *18* (73), 193−335.
(13) Pease, R. *Acta Crystallogr.* **1952**, *5* (3), 356−361.
(14) Novoselov, K. S.; Jiang, D.; Schedin, F.; Booth, T. J.; Khotkevich, V. V.; Morozov, S. V.; Geim, A. K. *Proc. Natl. Acad. Sci. U.S.A.* **2005**, *102* (30), 10451−10453.
(15) Shen, Y. R. *Annu. Rev. Phys. Chem.* **1989**, *40* (1), 327−350.
(16) McGilp, J. F.; Weaire, D. L.; Patterson, C. H., *Epioptics: Linear and Nonlinear Optical Spectroscopy of Surfaces and Interfaces*; Springer-Verlag GmbH: Berlin, 1995.
(17) Reider, G. A.; Heinz, T. F., Second-Order Nonlinear Optical Effects at Surfaces and Interfaces: Recent Advances. In *Photonic Probes of Surfaces: Electromagnetic Waves*; Halevi, P., Ed.; Elsevier Science Limited: New York, 1995; Vol. 2.
(18) Wagoner, G. A.; Persans, P. D.; Van Wagenen, E. A.; Korenowski, G. M. *J. Opt. Soc. Am. B* **1998**, *15* (3), 1017−1021.
(19) Kumar, N.; Najmaei, S.; Cui, Q.; Ceballos, F.; Ajayan, P. M.; Lou, J.; Zhao, H. *Phys. Rev. B* **2013**, *87* (16), 161403.
(20) Zeng, H.; Liu, G.-B.; Dai, J.; Yan, Y.; Zhu, B.; He, R.; Xie, L.; Xu, S.; Chen, X.; Yao, W.; Cui, X. *Sci. Rep.* **2013**, 3.
(21) Malard, L. M.; Alencar, T. V.; Barboza, A. P. M.; Mak, K. F.; de Paula, A. M. *Phys. Rev. B* **2013**, *87* (20), 201401.
(22) Mak, K. F.; Lee, C.; Hone, J.; Shan, J.; Heinz, T. F. *Phys. Rev. Lett.* **2010**, *105* (13), 136805.
(23) Splendiani, A.; Sun, L.; Zhang, Y.; Li, T.; Kim, J.; Chim, C.-Y.; Galli, G.; Wang, F. *Nano Lett.* **2010**, *10* (4), 1271−1275.
(24) Gorbachev, R. V.; Riaz, I.; Nair, R. R.; Jalil, R.; Britnell, L.; Belle, B. D.; Hill, E. W.; Novoselov, K. S.; Watanabe, K.; Taniguchi, T.; Geim, A. K.; Blake, P. *Small* **2011**, *7* (4), 465−468.
(25) Murray Sargent, I.; Scully, M. O. *Laser Physics*; Perseus Books: New York, 1978.
(26) Bloembergen, N.; Pershan, P. S. *Phys. Rev.* **1962**, *128* (2), 606−622.
(27) The experimental data were collected over a range of angles within a 180° rotation of the sample. Since the measurement geometry requires equivalent SH signals under sample rotation by 180°, we have plotted the experimental data at angles of both θ and θ + 180°.
(28) Shen, Y. R. *The principles of nonlinear optics*; Wiley-Interscience: New York, 2003.
(29) Hagimoto, K.; Mito, A. *Appl. Opt.* **1995**, *34* (36), 8276−8282.
(30) Nikogosyan, D. N. *Nonlinear Optical Crystals: A Complete Survey*; Springer-Verlag, 2005.
(31) Beal, A. R.; Hughes, H. P. *J. Phys. C: Solid State Phys.* **1979**, *12* (5), 881.
(32) Ishii, T.; Sato, T. *J. Cryst. Growth* **1983**, *61* (3), 689−690.
(33) Shi, Y.; Zhou, W.; Lu, A.-Y.; Fang, W.; Lee, Y.-H.; Hsu, A. L.; Kim, S. M.; Kim, K. K.; Yang, H. Y.; Li, L.-J.; Idrobo, J.-C.; Kong, J. *Nano Lett.* **2012**, *12* (6), 2784−2791.
(34) Lee, Y.-H.; Zhang, X.-Q.; Zhang, W.; Chang, M.-T.; Lin, C.-T.; Chang, K.-D.; Yu, Y.-C.; Wang, J. T.-W.; Chang, C.-S.; Li, L.-J.; Lin, T.-W. *Adv. Mater.* **2012**, *24* (17), 2320−2325.
(35) Zhan, Y.; Liu, Z.; Najmaei, S.; Ajayan, P. M.; Lou, J. *Small* **2012**, *8* (7), 966−971.
(36) Liu, K.-K.; Zhang, W.; Lee, Y.-H.; Lin, Y.-C.; Chang, M.-T.; Su, C.-Y.; Chang, C.-S.; Li, H.; Shi, Y.; Zhang, H.; Lai, C.-S.; Li, L.-J. *Nano Lett.* **2012**, *12* (3), 1538−1544.